Yeast
Yeast 2006; **23**: 389–398.
Published online in Wiley InterScience (www.interscience.wiley.com). **DOI:** 10.1002/yea.1363

Yeast Functional Analysis Report

Involvement of yeast *YOL151W/GRE2* in ergosterol metabolism

Jonas Warringer* and Anders Blomberg
Department of Cell and Molecular Biology, Lundberg Laboratory, Göteborg University Medicinaregatan 9c, 41390 Göteborg, Sweden

**Correspondence to:*
Jonas Warringer, Department of Cell and Molecular Biology, Lundberg Laboratory, Göteborg University Medicinaregatan 9c, 41390 Göteborg, Sweden.
E-mail:
Jonas.Warringer@gmm.gu.se

Received: 2 December 2005
Accepted: 31 January 2006

Abstract

The *Saccharomyces cerevisiae* gene *YOL151W/GRE2* is widely used as a model gene in studies on yeast regulatory responses to osmotic and oxidative stress. Nevertheless, information concerning the physiological role of this enzyme, a distant homologue of mammalian 3-β-hydroxysteroid dehydrogenases, is scarce. Combining quantitative phenotypic profiling and protein expression analysis studies, we here report the involvement of yeast Gre2p in ergosterol metabolism. Growth was significantly and exclusively reduced in *gre2*Δ strains subjected to environmental stress straining the cell membrane. Furthermore, whereas no compensatory mechanisms were activated due to loss of Gre2p during growth in favourable conditions (synthetic defined media, no stress), a striking and highly specific induction of the ergosterol biosynthesis pathway, represented by the enzymes Erg10p, Erg19p and Erg6p, was observed in *gre2*Δ during growth in a stress condition in which lack of Gre2p significantly affects growth. Involvement of Gre2p in ergosterol metabolism was confirmed by application of an array of selective inhibitors of lipid biosynthesis, as *gre2*Δ displayed vastly impaired tolerance exclusively to agents targeting the ergosterol biosynthesis. The approach outlined here, combining broad-spectrum phenotypic profiling, expression analysis during conditions reducing the growth of the mutant and functional confirmation by application of highly selective inhibitors, may prove a valuable tool in gene functional analysis.

Keywords: **GRE2; phenotypic profiling; ergosterol; steroid metabolism**

Introduction

Global expression patterns induced by gene disruption may reveal compensatory mechanisms initiated by the cell to cope with the loss of gene function. However, loss of individual genes generally does not provoke fundamental changes in regulation patterns during conditions of little environmental stress (Hughes *et al*., 2000), suggesting that compensatory mechanisms are not induced because the deleted gene is of little importance during optimal conditions. Hence, a prerequisite for finding relevant compensatory regulatory mechanisms may be initial phenotypic screening in a wide spectrum of stressful environments to reveal conditions in which lack of Gre2p significantly affects growth.

This principle is here illustrated by the functional dissection of the stress-induced gene *YOL151W/GRE2* (genes de respuesta a estres, 'stress-responsive gene', Spanish), a member of a family of four unclassified but highly conserved open reading frames in *S. cerevisiae* (Garay-Arroyo and Covarrubias, 1999; Hajji *et al*., 1999). Much is known about *GRE2* regulation; in fact, the remarkably strong induction of the *GRE2* promotor in a variety of stresses, such as osmotic and oxidative stress (Garay-Arroyo and Covarrubias, 1999), has made it a model gene in research on stress activation (Van Wuytswinkel *et al*., 2000). (a) Induction of *GRE2* during osmotic stress conditions has been shown to be dependent on two CRE (cAMP response element) promoter elements acted upon by the bZIP transcription factor Sko1p (Rep *et al*., 2001), a downstream target of the HOG (high osmolarity glycerol) signalling pathway in yeast (Proft and Serrano, 1999). (b) Osmotic

stress activation of *GRE2* is higher in aerobic than anaerobic conditions (Krantz *et al*., 2004). (c) Oxidative stress activation of *GRE2* is independent of Sko1p but dependent on the AP1-like transcription factor Yap1p (Rep *et al*., 2001), a dominant regulator of the oxidative stress response in yeast (Stephen *et al*., 1995). (d) Basal expression of *GRE2* appears to be an interplay between Yap1p, Sko1p and two other CRE binding transcription factors Aca1p and Aca2p (Rep *et al*., 2001). (e) The metal responsive transcription factor Zap1p (Rutherford and Bird, 2004) and the histone deacetylase complex component Rpd3p (De Nadal *et al*., 2004) have been reported to act upon the *GRE2* promotor.

In stark contrast to the abundance of information concerning *GRE2* regulation, very little is known about Gre2p function. Gre2p has been shown to possess low-affinity methylglyoxal reductase activity (Chen *et al*., 2003) as well as low-affinity stereo-selective ability to reduce the carbonyl compound ethyl acetoacetate (Katz *et al*., 2003). However, whether these activities are physiologically relevant and relate to the true biological role of Gre2p is currently unclear. Here we show that loss of Gre2p, although of no importance during growth in favourable conditions (synthetic defined media, no stress), results in stress phenotypes indicative of cell membrane defects. Furthermore, whereas no compensatory mechanisms were activated in the deletion strain during growth in favourable conditions, specific and exclusive induction of Erg6p, Erg10p and Erg19p in the ergosterol biosynthesis pathway was observed when *gre2*Δ was exposed to conditions in which lack of Gre2p significantly affected growth. Finally, applying a plethora of agents selectively targeting specific enzymes in lipid biosynthesis, we show that loss of Gre2p confers hypersensitivity to ergosterol biosynthesis disrupting agents, confirming a role of Gre2p in ergosterol biosynthesis.

Materials and methods

Yeast strains

Strains used were generated through the EUROSCARF project as derivatives of the FY1679 strain and provided by the EUROSCARF stock center (**http://www.uni-frankfurt.de/fb15/mikro/euroscarf/index.html**) as haploids; wide-type genotype; *matα*, *ura3-52, trp1-Δ63, leu2Δ1*; *Gre2*Δ genotype; *matα*, *ura3-52, trp1-Δ63, leu2Δ1*,*YOL151W(4, 877)::kanMX4*. Strains were long-time stored in 20% glycerol at −80 °C and pre-experimentally stored at +4 °C on agar slopes.

Media and growth conditions

Pre-cultures were incubated overnight (approximately 24 h) at 30 °C on a rotary shaker in 5 ml SD medium (2% w/v glucose, 0.14% yeast nitrogen base without amino acids (YNB; Difco), 0.5% ammonium sulphate and 1% succinic acid, supplemented with 20 mg/l uracil, 20 mg/l tryptophan, 20 mg/l histidine and 100 mg/l leucine, pH 5.8) in 15 ml tubes. Pre-cultures were washed in milliQ water and inoculated to OD = 0.07–0.1 in fresh SD media (as above) in 100-well honeycomb plates, 350 µl in each well. Conditions of environmental stress were as follows: methylviologen (paraquat) 167, 84, 42 µg/ml, menadione (0.1, 0.03, 0.006 mM), benomyl (50, 10, 1 µg/ml), ethanol (6%, 5%, 4%), 4-NQO (0.007, 0.0035, 0.001 µg/ml), cycloheximide (0.03, 0.01, 0.001 µg/ml), hydroxyurea (15, 6, 2 mg/ml), tunicamycin (2, 0.5, 0.1 µg/ml), hygromycin B (0.25, 0.1, 0.025 mg/ml), rapamycin (0.05, 0.025, 0.01 µg/ml), 1,10 phenanthroline (0.01, 0.005, 0.0025 mM), caffeine (1.5, 1, 0.5 mg/ml), compound 48/80 (10, 5, 2.5 µg/ml), calcofluor white (2, 0.4, 0.08 mg/ml), DNP (0.2, 0.1, 0.05 mg/ml), SDS (0.01%, 0.0075%, 0.005%), cytochalasin D (5, 2.5, 1 µg/ml), trifluoperazine (12.5, 10, 7.5 µM), canavanine (10, 5, 1 µg/ml), diamide (1, 0.75, 0.5 mM), $CdCl_2$(5, 2 µg/ml), neomycin sulphate (35, 18, 9 mM), $CaCl_2$ (500, 150, 50 mM), NaCl (1.0, 0.75, 0.5 mM), sorbitol (1, 0.75, 0.5 mM), EGTA (30, 15, 7.5 mM), G418 (525, 262.5, 131.25 µg/ml), Brefeldin A (890, 445, 100 µM), AT-3 (175, 131.25, 87.5 mM), camptothecin (120, 90, 60 µg/ml), 2,3-DPG (12.5, 6.25, 1 mM), ethidiumbromide (180, 90, 45 µg/ml), vanadium (6, 3.75 mM), coerulenin (0.125, 0.25, 0.5 µg/ml), myriocin (10, 15, 20 µg/ml), aureobasidin A (0.125, 0.25, 0.5 µg/ml), fumonisin B_1 (50, 100, 200 µM), mevinolin (125, 250, 500 µg/ml) fenpropimorph (120, 240, 480 µg/ml), ketoconazole (62.5, 125, 250 µM), clotrimazole (1.5, 15, 100 µM) and amphotericin B (12.5, 25, 50 µg/ml). All chemicals were obtained at the highest available

grade (Sigma-Aldrich, USA; except for aureobasidin A, Takara Shuzo Ltd, Japan).

Measurement of growth

Optical density was recorded using a Bioscreen Analyzer C (Growth Curve Oy, Finland) as reported previously (Warringer and Blomberg, 2003). Experimental temperatures were kept at 30 °C except for during heat stress at 40 °C, 41 °C or 42 °C. Strains were tested in duplicate or, in the case of the final test of lipid biosynthesis inhibitors, in triplicate, with *gre2*Δ strains and reference strains on separate plates but with reference conditions (no stress, favourable conditions) in triplicate on all plates and used as internal standards. Adaptation time, rate of growth and efficiency of growth was calculated as indicated earlier, as were the corresponding strain coefficients (SCs) and phenotypical indices (PIs) (Warringer and Blomberg, 2003).

High resolution 2D-PAGE

Strains were microcultivated in SD media (as above) in triplicate, with and without 15 mM EGTA to mid-exponential phase ($7-8 \times 10^6$ cells/ml) and labelled with 0.14 μCi [^{35}S] methionine/well for a time proportional to their growth rate (reference strain growing in absence of stress was labelled for 30 min). Growth was terminated by transferring cultures to microcentrifuge tubes on ice. Subsequent preparation of cell extracts and determination of incorporated radioactivity was performed as previously reported (Blomberg *et al*., 1995). Isoelectric focusing, second-dimensional separation and image analysis was performed as in (Norbeck and Blomberg, 1997); >600 protein spots were matched in all gels and significant expression changes were identified (> two-fold change; Student's *t*-test, $p < 0.05$). Identifications of proteins were accomplished using reference 2D patterns from MALDI–TOF experiments performed previously (Norbeck and Blomberg, 1997; and unpublished data).

Results

GRE2 is a homologue of mammalian 3-β-hydroxysteroid dehydrogenases

Sequence homology searches identified Gre2p as a member of a tightly conserved family of proteins in *S. cerevisiae*, also containing the functionally unclassified Ygl39wp, Ydr541cp and Ygl157wp (Hajji *et al*., 1999). No firm experimental data are available regarding the function of these proteins. Sequence identity to Gre2p within the *GRE2* family corresponds to 55–60% (BlastP) over the full-length proteins. Clear Gre2p orthologues are also present throughout yeast, as illustrated by occurrence in *Schizosaccharomyces pombe, Zygosaccharomyces rouxii* and *Candida albicans* (Figure 1). Gre2p displays significant sequence identity, 30–36% over the full-length protein, to a family of plant dihydroflavonol 4-reductases (Figure 1) catalysing reactions involved in the detoxification of flavonoid compounds (Hayashi *et al*., 2005). We also find indications as to the function of Gre2p in the sequence identity, 27–31% over 210–270 amino acids (full-length

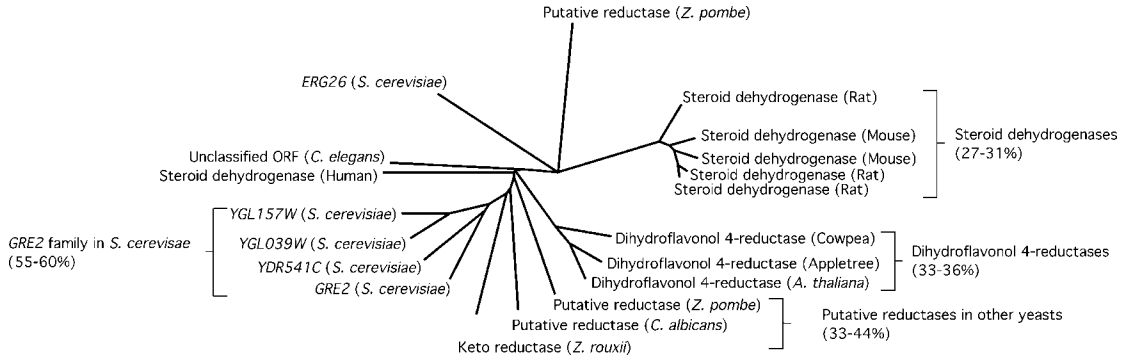

Figure 1. *GRE2* is a homologue of mammalian 3-β-hydroxysteroid dehydrogenases. Multiple sequence alignments of Gre2p homologues were performed, using ClustalW (Thompson *et al*., 1994), and visualized as an unrooted tree, using Treeview (Page, 1996). BlastP sequence identity to Gre2p is indicated

Gre2p = 342 amino acids), of Gre2p to a family of mammalian 3-β-hydroxysteroid dehydrogenases functioning in the interconversion of steroid precursors in steroid biosynthesis (Lachance *et al*., 1990). In addition, the C-3 sterol dehydrogenase in *S. cerevisiae,* Erg26p (Gachotte *et al*., 1998), shares 25% sequence identity over 276 amino acids with *GRE2*, and is the closest *S. cerevisiae* homologue to Gre2p outside the Gre2p group (Figure 1). Evolutionary relationship thus implicates Gre2p as a probable reductase involved in flavonol and steroid metabolism.

Gre2p is dispensable during favourable conditions

Investigating, by differential display proteomics, the expression changes induced in *gre2*Δ during exponential growth in favourable conditions (synthetic defined media, no stress), we found no compensatory mechanisms to be induced (data not shown). To deduce whether this lack of compensatory gene activation is due to an absolute dispensability of the gene in conditions with low levels of external stress, we measured the growth phenotype in strains lacking Gre2p during these conditions. We have previously introduced a methodology for the precise quantification of marginal growth defects in *S. cerevisiae* deletion strains (Warringer and Blomberg, 2003). Growth in a particular environment is measured in relation to the behaviour of the wild-type strain. Quantifying the growth behaviour of *gre2*Δ in favourable conditions we found no phenotypic defect, considering either the time to initiate growth (adaptation time), the rate of exponential growth (growth rate) or the efficiency of growth (population density reached). Hence, the lack of compensatory gene activation may be due to full dispensability of Gre2p in conditions favourable for growth.

Loss of *GRE2* confers growth rate defects during cell membrane stress

To identify conditions in which lack of Gre2p significantly affects growth and in which loss of Gre2p function may induce compensatory gene regulatory mechanisms, the growth behaviour of *gre2*Δ was profiled during 32 environmental stresses. These stresses were chosen to affect a wide diversity of features of yeast physiology. Each environmental stress was represented by three concentrations, selected to represent low (25–50% increase in generation time), medium (50–100% increase in generation time) and high (100–200% increase in generation time) levels of growth inhibition on the reference strain (see Materials and methods). Specific gene–environment interactions were obtained by comparing the strain coefficient of *gre2*Δ in each environment to the strain coefficient in normal (unstressed) conditions, forming phenotypic indices (PIs) as described previously (Warringer *et al*., 2003). A high PI (>1) indicates resistance of *gre2*Δ to the environmental stress in question, whereas a low PI (<1) indicates a growth defect. We found that *gre2*Δ displayed several substantial growth defects during environmental stress (Figure 2). The majority of these growth defects were concentration-dependent; most frequently the higher the environmental stress applied, the more pronounced the specific growth defects of strains lacking Gre2p (Figure 2). Prominent among the rate of growth phenotypes were growth deficiencies during conditions of saline stress (NaCl) and conditions of decreased levels of calcium ions (EGTA). The latter agent is reported to affect ergosterol biosynthesis (Cronin *et al*., 2000). The observed sensitivity of *gre2*Δ to EGTA, linking Gre2p to ergosterol production, is in line with the pronounced growth deficiencies of *gre2*Δ in the presence of the cell membrane-perturbing agent SDS and in the presence of hygromycin B (Figure 2), agents specifically used in probing for cell envelope defects (Lussier *et al*., 1997; Santos and Snyder, 2000).

Reduced growth efficiency in *gre2*Δ when membrane trafficking is disrupted

Frequently, aberrant growth behaviour of a deletion strain is exclusive for a single growth variable, e.g. growth rate deficiencies are not reflected in similar adaptation time or growth efficiency deficiencies (Warringer *et al*., 2003). In the case of *gre2*Δ, the growth rate phenotypes observed in the presence of EGTA, NaCl, SDS and hygromycin B were matched by similar growth efficiency phenotypes (data not shown). However, an exclusive growth efficiency defect during treatment with Brefeldin A (Figure 3) was also found. Brefeldin A interferes with the trafficking of membrane components by inhibition of a Golgi-associated guanine nucleotide exchange protein (Sata *et al*., 1999)

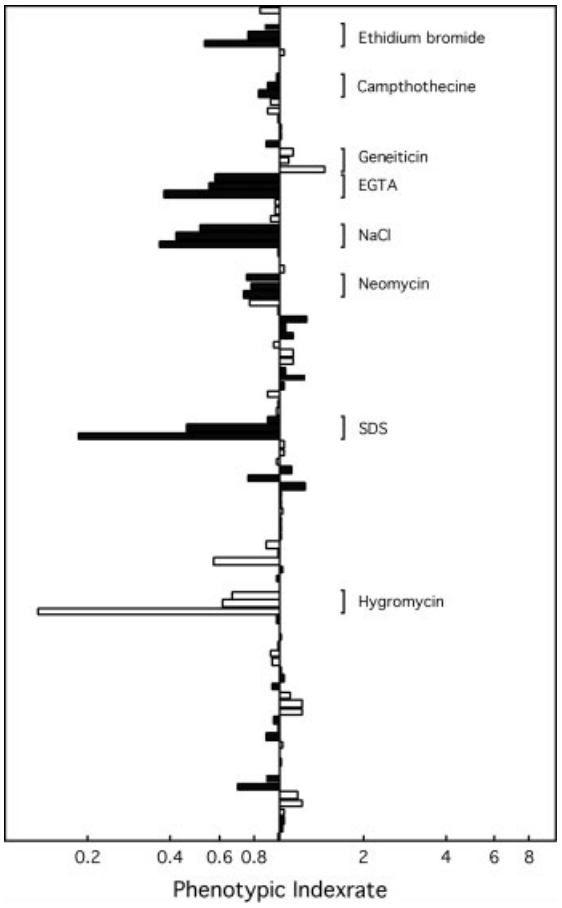

Figure 2. Loss of *GRE2* confers growth rate defects during cell membrane stress. *gre2*Δ growth rate phenotypes were determined using a wide array of environmental stresses. Three concentrations of each environmental agent were used, the highest concentration being the lowermost of the three bars (for a complete list of agents and concentrations, see Materials and methods). For easier visualization, environmental agents were alternately coloured in black and white

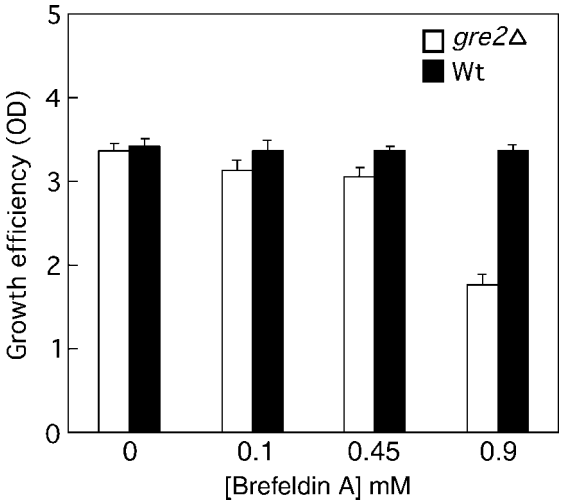

Figure 3. Reduced growth efficiency in *gre2*Δ when membrane trafficking is disrupted. Growth efficiency of *gre2*Δ in the presence of different concentrations of Brefeldin A as compared to the reference strain

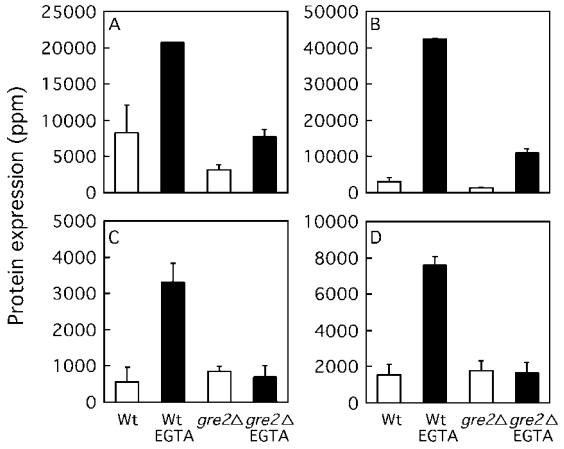

Figure 4. Compromised induction of stress genes in *gre2*Δ during stress. Relative protein expression (2D-PAGE) of: (A) Eno1p; (B) Tdh1p; (C) Hxk1p; (D) Rnr4p in wild-type and *gre2*Δ cells in response to treatment with 15 mM EGTA

and decreased Brefeldin A tolerance is generally observed for strains deleted for ergosterol biosynthesis components, such as Erg6p (Shah and Klausner, 1993) and Erg4p (Zweytick *et al*., 2000). Thus, the Brefeldin A efficiency defects of *gre2*Δ are in line with Gre2p being involved in ergosterol metabolism.

Loss of *GRE2* function results in stress-dependent induction of ergosterol biosynthesis

To investigate whether any compensatory mechanisms are activated in response to loss of *GRE2* function in conditions where lack of Gre2p significantly affects growth, the protein expression pattern of *gre2*Δ strain cultivated in the presence and absence of EGTA was investigated using 2D-PAGE. In wild-type cells, addition of EGTA evoked a shift in protein expression patterns, largely consistent with the general stress response (Causton *et al*., 2001; Gasch *et al*., 2000). However, the induction of most of the prominent general stress response proteins, notably Eno1p, Tdh1p, Rnr4p and Hxk1p (Figure 4), was severely

compromised in the *gre2*Δ strain cultivated in EGTA. This suggests that the molecular basis for the stress-related growth deficiencies of *gre2*Δ may be coupled to its defect in the initiation of the general stress response. We also found a distinct and gene-specific induction of proteins involved in the biosynthesis of cell membrane/cell wall components in *gre2*Δ cultivated in EGTA. Of the four identified proteins induced in *gre2*Δ in EGTA, three were components of the ergosterol biosynthesis pathway, Erg10p, Erg6p and Erg19p, whereas the fourth, Bgl2p, is a β-glucan synthesis protein involved in cell wall biogenesis (Figure 5). This compensatory activation of the ergosterol biosynthesis pathway in *gre2*Δ in response to EGTA treatment suggests that *gre2*Δ cells experience shortage of ergosterol when facing Ca^{2+} depletion.

Confirmation of the Gre2p-ergosterol link by use of selective ergosterol biosynthesis inhibitors

A function for Gre2p in steroid metabolism or in ergosterol assembly into membranes is indicated

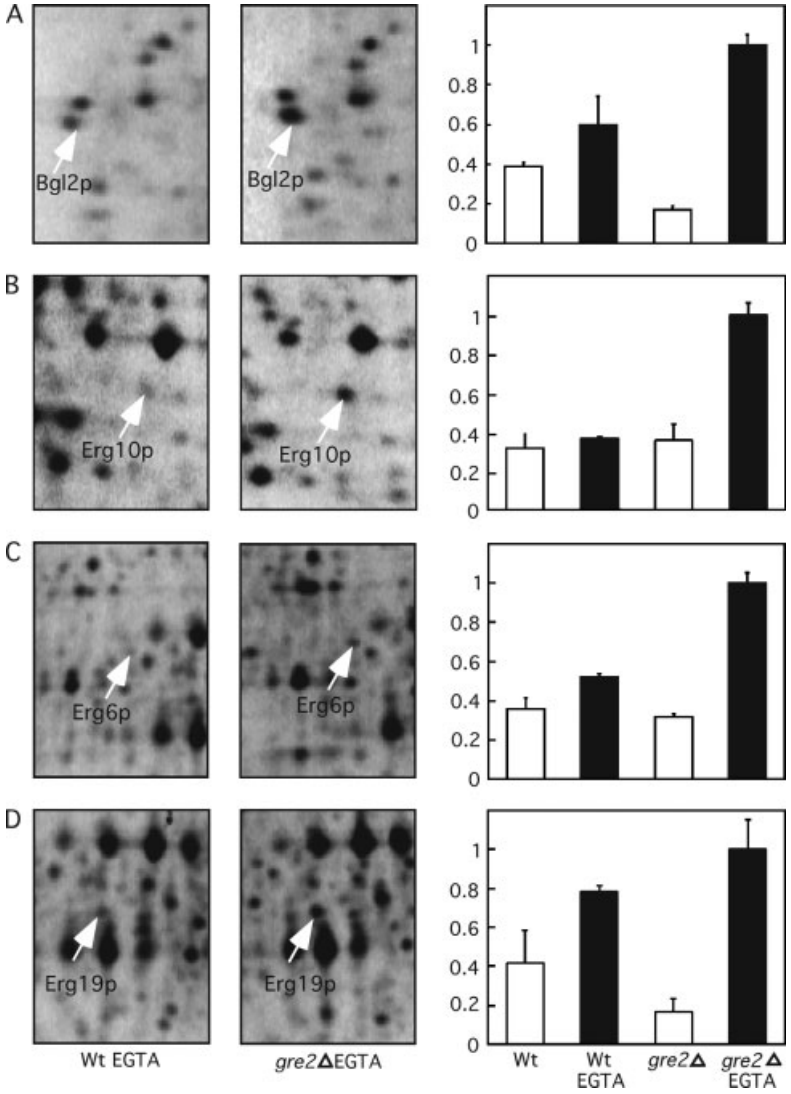

Figure 5. Loss of *GRE2* function results in stress-dependent induction of ergosterol biosynthesis. Relative protein expression (2D-PAGE) of: (A) Bgl2p; (B) Erg10p; (C) Erg6p; (D) Erg19p in wild-type and *gre2*Δ in response to treatment with 15 mM EGTA. Error bars indicate standard deviations. The expression of each protein in *gre2*Δ in EGTA was set to 1

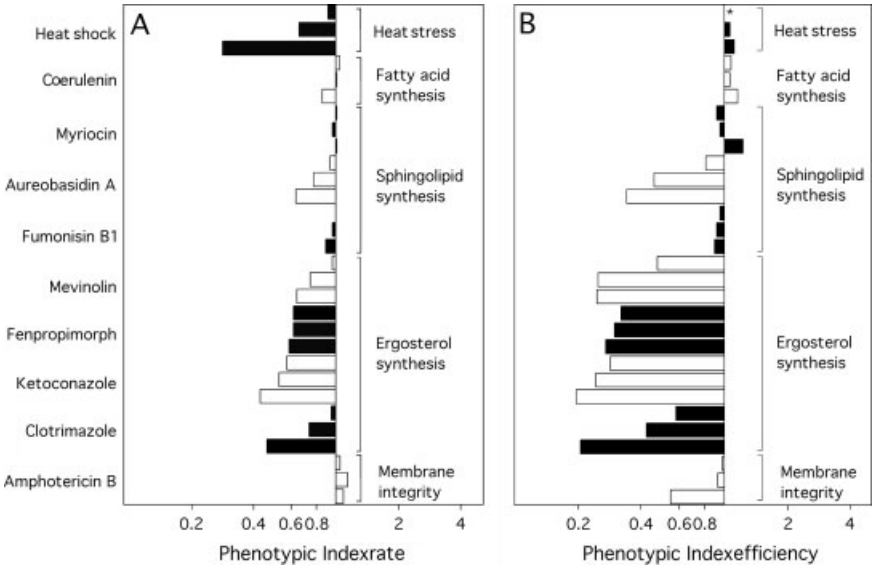

Figure 6. Loss of *GRE2* confers reduced tolerance to selective ergosterol biosynthesis inhibitors. Phenotypic behaviour of *gre2*Δ during environmental stress induced by lipid biosynthesis inhibitors, considering (A) growth rate and (B) growth efficiency. Three concentrations of each environmental agent were used, the highest concentration being the lowermost of the three bars

by: (a) sequence similarity of Gre2p to mammalian 3-β-hydroxysteroid dehydrogenases; (b) specific sensitivity of strains lacking Gre2p to cell membrane/cell wall perturbation; and (c) compensatory activation of ergosterol biosynthesis genes in *gre2*Δ during stress that affects the cell membrane composition. To confirm these indications, the growth behaviour of *gre2*Δ in the presence of nine very selective inhibitors of lipid biosynthesis, including four ergosterol biosynthesis inhibitors, was investigated. We found that *gre2*Δ displayed normal growth behaviour in the presence of the fatty acid biosynthesis inhibitor coerulenin (Figure 6A, B). A moderate sensitivity to aureobasidin A was observed; however, *gre2*Δ displayed normal growth behaviour in the presence of the other sphingolipid biosynthesis inhibitors, myriocin and fumonisin B_1. Aureobasidin A, in deference to myriocin and fumonisin B_1, inhibits one of the later stages in sphingolipid biosynthesis, below the enzymatic steps where extensive cross-talk between ergosterol and sphingolipid biosynthesis is assumed to occur (reviewed in Veen and Lang, 2005). In sharp contrast to the minor effects when inhibiting fatty acid or sphingolipid biosynthesis, we found very pronounced defects in the tolerance to all the inhibitors of ergosterol biosynthesis tested (Figure 6): clotrimazole and ketoconazole inhibiting Erg11p, fenpropimorph inhibiting Erg24p and Erg2p, and mevinolin inhibiting Hmg1p and Hmg2p. Hence, irrespective of where the ergosterol biosynthesis pathway was blocked, *gre2*Δ displayed severe deficiencies. Although these ergosterol biosynthesis phenotypes were also significant at the level of growth rate (Figure 6A), they were most pronounced considering growth efficiency (Figure 6B), implicating increased expenditure of ATP or reducing power as the underlying cause. This is supported by the observation that g*re2*Δ has an exclusive growth efficiency defect in the presence of amphotericin B, an agent (Figure 6B) selectively binding to ergosterol in the cell membrane, thereby affecting membrane fluidity (Bennett, 1996). The pronounced and consistent efficiency defects of g*re2*Δ in the presence of agents disturbing ergosterol-related processes indicates defects in cell membrane integrity that result in enhanced costs of maintaining cellular homeostasis in g*re2*Δ.

Discussion

In this article a functional investigation of the stress-induced gene *GRE2* was performed

by combining broad array phenotypic profiling, expression analysis and the final application of selective growth inhibitors. We found strains deleted for Gre2p to be highly and specifically sensitive to stress induced by EGTA, SDS, NaCl, hygromycin and Brefeldin A, agents which severely strain cell membrane-related processes. In particular, this is valid for EGTA, a chelator of divalent ions with high Ca^{2+} specificity, as calcium has been documented to be an essential secondary messenger for signalling pathways related to cell integrity (Carnero *et al*., 2000). In addition, it is known that disturbances in cell integrity increase the cellular importance of ergosterol metabolism-related genes and results in enhanced ergosterol content in yeast cell membranes (Jung *et al*., 2005; Shah and Klausner, 1993; Welihinda *et al*., 1994; Zweytick *et al*., 2000). An interesting, novel link between ergosterol and calcium is the enhanced calcium requirement of strains such as *erg6*Δ (Adler L, Forsmark A, personal communication) with disturbed ergosterol biosynthesis.

Further support for a link between *GRE2* and ergosterol metabolism was provided by the increased sensitivity of the *gre2*Δ strain to specific inhibitors of ergosterol biosynthesis. These agents, mevinolin, fenpropimorph, clotrimazole and ketoconazole, selectively inhibit enzymes in ergosterol biosynthesis. Hence, the *gre2*Δ phenotypes can be directly linked to a decrease in ergosterol production. It is noteworthy that impaired ergosterol biosynthesis, e.g. as achieved by the addition of azoles, is reported to affect Ca^{2+} influx and depletes intracellular Ca^{2+} stores (Alvarez *et al*., 1992; Benzaquen *et al*., 1995), thus mimicking the actions of EGTA. The link to ergosterol metabolism was strengthened by the specific compensatory production of Erg10p, catalysing the initial step of the mevalonate–ergosterol synthesis pathway, Erg19p, a mevalonate pyrophosphate decarboxylase, and Erg6p, a C-24 methyltransferase, in EGTA-stressed *gre2*Δ cells. However, as analysis of most Erg proteins is currently not possible by 2D-PAGE, regulation of Erg proteins other than Erg6p, Erg10p and Erg19p cannot be excluded. We also note that sequence similarity implicates Gre2p as a distant homologue of a family of mammalian 3-β-hydroxysteroid dehydrogenases providing a further indication linking Gre2p to ergosterol metabolism. Such a link is supported by the substantial induction of *GRE2* to both chemical perturbations of the ergosterol biosynthesis pathway (Bammert and Fostel, 2000) using a multitude of azole compounds, and to various genetic manipulations of *PDR5* and *PDR1* in the multidrug response (DeRisi *et al*., 2000). Importantly, these previous expression profiling studies group *GRE2* in tight clusters, specifically and markedly enriched for ergosterol metabolism genes. The characterization of additional genes related to ergosterol metabolism in yeast is of general interest, as this pathway is the prime target for antifungal agents.

Gre2p has recently been reported to possess weak methylglyoxal reductase activity (Chen *et al*., 2003), a feature most commonly associated with aldehyde/alcohol dehydrogenases, e.g. Adh1p, with no sequence similarity to Gre2p. However, no such methylglyoxal reductase activity was found for the three highly conserved *S. cerevisiae* homologues of Gre2p (Chen *et al*., 2003). Furthermore, the methylglyoxal reductase activity reported by Chen *et al*. (2003) was observed only at a high substrate concentration (10 mM methylglyoxal). Hence, it cannot be excluded that the reported methylglyoxal reductase activity results from cross-reactivity and does not reveal the native substrate for the enzyme. The strong sequence similarity to dihydroflavonol dehydrogenases in plants indicates that methylglyoxal is not the preferred substrate of Gre2p; rather, the common ring structure of flavonols and steroids indicates that these compounds may indeed be more optimal Gre2p substrates. In concert with the sequence similarity to flavonol reductases, our experimental data support the possibility that Gre2p could be a broad specificity reductase, mainly acting in ergosterol metabolism in yeast with various steroid derivatives as substrates. Broad specificity has been reported for a large number of dehydrogenase enzymes in yeast, e.g. NADPH-dependent alcohol dehydrogenase, YCR105W (Larroy *et al*., 2002). It should be noted that many of the intermediates of ergosterol biosynthesis has been reported as toxic to yeast and constitute possible native targets for the detoxification capability of Gre2p.

References

Alvarez J, Montero M, Garcia-Sancho J. 1992. High affinity inhibition of Ca(2+)-dependent K+ channels by cytochrome P-450 inhibitors. *J Biol Chem* **267**: 11 789–11 793.

Bammert GF, Fostel JM. 2000. Genome-wide expression patterns in *Saccharomyces cerevisiae*: comparison of drug treatments and genetic alterations affecting biosynthesis of ergosterol. *Antimicrob Agents Chemother* **44**: 1255–1265.

Bennett JE. 1996. Antimicrobial agents (antifungal agents). In *Goodman and Gilman's The Pharmacological Basis of Therapeutics*, Hardman JG, Limbird LE, Molinoff PB, Ruddon RW, Gilman AG (eds). McGraw-Hill: New York; 1175–1188.

Benzaquen LR, Brugnara C, Byers HR, Gatton-Celli S, Halperin JA. 1995. Clotrimazole inhibits cell proliferation *in vitro* and *in vivo*. *Nat Med* **1**: 534–540.

Blomberg A, Blomberg L, Norbeck J, *et al*. 1995. Interlaboratory reproducibility of yeast protein patterns analyzed by immobilized pH gradient two-dimensional gel electrophoresis. *Electrophoresis* **16**: 1935–1945.

Carnero E, Ribas JC, Garcia B, Duran A, Sanchez Y. 2000. *Schizosaccharomyces pombe* ehs1p is involved in maintaining cell wall integrity and in calcium uptake. *Mol Gen Genet* **264**: 173–183.

Causton HC, Ren B, Koh SS, *et al*. 2001. Remodeling of yeast genome expression in response to environmental changes. *Mol Biol Cell* **12**: 323–337.

Chen CN, Porubleva L, Shearer G, *et al*. 2003. Associating protein activities with their genes: rapid identification of a gene encoding a methylglyoxal reductase in the yeast *Saccharomyces cerevisiae*. *Yeast* **20**: 545–554.

Cronin SR, Khoury A, Ferry DK, Hampton RY. 2000. Regulation of HMG-CoA reductase degradation requires the P-type ATPase Cod1p/Spf1p. *J Cell Biol* **148**: 915–924.

De Nadal E, Zapater M, Alepuz PM, *et al*. 2004. The MAPK Hog1 recruits Rpd3 histone deacetylase to activate osmoresponsive genes. *Nature* **427**: 370–374.

DeRisi J, van den Hazel B, Marc P, *et al*. 2000. Genome microarray analysis of transcriptional activation in multidrug resistance yeast mutants. *FEBS Lett* **470**: 156–160.

Gachotte D, Barbuch R, Gaylor J, Nickel E, Bard M. 1998. Characterization of the *Saccharomyces cerevisiae ERG26* gene encoding the C-3 sterol dehydrogenase (C-4 decarboxylase) involved in sterol biosynthesis. *Proc Natl Acad Sci USA* **95**: 13 794–13 799.

Garay-Arroyo A, Covarrubias AA. 1999. Three genes whose expression is induced by stress in *Saccharomyces cerevisiae*. *Yeast* **15**: 879–892.

Gasch AP, Spellman PT, Kao CM, *et al*. 2000. Genomic expression programs in the response of yeast cells to environmental changes. *Mol Biol Cell* **11**: 4241–4257.

Hajji K, Clotet J, Arino J. 1999. Disruption and phenotypic analysis of seven ORFs from the left arm of chromosome XV of *Saccharomyces cerevisiae*. *Yeast* **15**: 435–441.

Hayashi M, Takahashi H, Tamura K, *et al*. 2005. Enhanced dihydroflavonol-4-reductase activity and NAD homeostasis leading to cell death tolerance in transgenic rice. *Proc Natl Acad Sci USA* **102**: 7020–7025.

Hughes TR, Marton MJ, Jones AR, *et al*. 2000. Functional discovery via a compendium of expression profiles. *Cell* **102**: 109–126.

Jung WH, Warn P, Ragni E, *et al*. 2005. Deletion of *PDE2*, the gene encoding the high-affinity cAMP phosphodiesterase, results in changes of the cell wall and membrane in *Candida albicans*. *Yeast* **22**: 285–294.

Katz M, Frejd T, Hahn-Hagerdal B, Gorwa-Grauslund MF. 2003. Efficient anaerobic whole cell stereoselective bioreduction with recombinant *Saccharomyces cerevisiae*. *Biotechnol Bioeng* **84**: 573–582.

Krantz M, Nordlander B, Valadi H, *et al*. 2004. Anaerobicity prepares *Saccharomyces cerevisiae* cells for faster adaptation to osmotic shock. *Eukaryot Cell* **3**: 1381–1390.

Lachance Y, Luu-The V, Labrie C, *et al*. 1990. Characterization of human 3-β-hydroxysteroid dehydrogenase/Δ 5-Δ4-isomerase gene and its expression in mammalian cells. *J Biol Chem* **265**: 20 469–20 475.

Larroy C, Fernandez MR, Gonzalez E, Pares X, Biosca JA. 2002. Characterization of the *Saccharomyces cerevisiae* YMR318C (*ADH6*) gene product as a broad specificity NADPH-dependent alcohol dehydrogenase: relevance in aldehyde reduction. *Biochem J* **361**: 163–172.

Lussier M, White AM, Sheraton J, *et al*. 1997. Large scale identification of genes involved in cell surface biosynthesis and architecture in *Saccharomyces cerevisiae*. *Genetics* **147**: 435–450.

Norbeck J, Blomberg A. 1997. Two-dimensional electrophoretic separation of yeast proteins using a non-linear wide range (pH 3–10) immobilized pH gradient in the first dimension; reproducibility and evidence for isoelectric focusing of alkaline (pI > 7) proteins. *Yeast* **13**: 1519–1534.

Page RD. 1996. TreeView: an application to display phylogenetic trees on personal computers. *Comput Appl Biosci* **12**: 357–358.

Proft M, Serrano R. 1999. Repressors and upstream repressing sequences of the stress-regulated *ENA1* gene in *Saccharomyces cerevisiae*: bZIP protein Sko1p confers HOG-dependent osmotic regulation. *Mol Cell Biol* **19**: 537–546.

Rep M, Proft M, Remize F, *et al*. 2001. The *Saccharomyces cerevisiae* Sko1p transcription factor mediates HOG pathway-dependent osmotic regulation of a set of genes encoding enzymes implicated in protection from oxidative damage. *Mol Microbiol* **40**: 1067–1083.

Rutherford JC, Bird AJ. 2004. Metal-responsive transcription factors that regulate iron, zinc, and copper homeostasis in eukaryotic cells. *Eukaryot Cell* **3**: 1–13.

Santos B, Snyder M. 2000. Sbe2p and sbe22p, two homologous Golgi proteins involved in yeast cell wall formation. *Mol Biol Cell* **11**: 435–452.

Sata M, Moss J, Vaughan M. 1999. Structural basis for the inhibitory effect of brefeldin A on guanine nucleotide-exchange proteins for ADP-ribosylation factors. *Proc Natl Acad Sci USA* **96**: 2752–2757.

Shah N, Klausner RD. 1993. Brefeldin A reversibly inhibits secretion in *Saccharomyces cerevisiae*. *J Biol Chem* **268**: 5345–5348.

Stephen DW, Rivers SL, Jamieson DJ. 1995. The role of the *YAP1* and *YAP2* genes in the regulation of the adaptive oxidative stress responses of *Saccharomyces cerevisiae*. *Mol Microbiol* **16**: 415–423.

Thompson JD, Higgins DG, Gibson TJ. 1994. CLUSTAL W: improving the sensitivity of progressive multiple sequence alignment through sequence weighting, position-specific gap penalties and weight matrix choice. *Nucleic Acids Res* **22**: 4673–4680.

Van Wuytswinkel O, Reiser V, Siderius M, *et al*. 2000. Response of *Saccharomyces cerevisiae* to severe osmotic stress: evidence

for a novel activation mechanism of the HOG MAP kinase pathway. *Mol Microbiol* **37**: 382–397.

Veen M, Lang C. 2005. Interactions of the ergosterol biosynthetic pathway with other lipid pathways. *Biochem Soc Trans* **33**: 1178–1181.

Warringer J, Blomberg A. 2003. Automated screening in environmental arrays allows analysis of quantitative phenotypic profiles in *Saccharomyces cerevisiae*. *Yeast* **20**: 53–67.

Warringer J, Ericson E, Fernandez L, Nerman O, Blomberg A. 2003. High-resolution yeast phenomics resolves different physiological features in the saline response. *Proc Natl Acad Sci USA* **100**: 15 724–15 729.

Welihinda AA, Beavis AD, Trumbly RJ. 1994. Mutations in LIS1 (*ERG6*) gene confer increased sodium and lithium uptake in *Saccharomyces cerevisiae*. *Biochim Biophys Acta* **1193**: 107–117.

Zweytick D, Hrastnik C, Kohlwein SD, Daum G. 2000. Biochemical characterization and subcellular localization of the sterol C-24(28) reductase, erg4p, from the yeast *Saccharomyces cerevisiae*. *FEBS Lett* **470**: 83–87.